



THE UNIVERSITY *of* EDINBURGH

Edinburgh Research Explorer

Sestrins induce natural killer function in senescent-like CD8+ T cells

Citation for published version:

Pereira, BI, De Maeyer, RPH, Covre, LP, Nehar-Belaid, D, Lanna, A, Ward, S, Marches, R, Chambers, ES, Gomes, DCO, Riddell, NE, Maini, MK, Teixeira, VH, Janes, SM, Gilroy, DW, Larbi, A, Mabbott, N, Ucar, D, Kuchel, GA, Henson, SM, Strid, J, Lee, JH, Banachereau, J & Akbar, AN 2020, 'Sestrins induce natural killer function in senescent-like CD8+ T cells', *Nature Immunology*. <https://doi.org/10.1038/s41590-020-0643-3>

Digital Object Identifier (DOI):

[10.1038/s41590-020-0643-3](https://doi.org/10.1038/s41590-020-0643-3)

Link:

[Link to publication record in Edinburgh Research Explorer](#)

Document Version:

Peer reviewed version

Published In:

Nature Immunology

General rights

Copyright for the publications made accessible via the Edinburgh Research Explorer is retained by the author(s) and / or other copyright owners and it is a condition of accessing these publications that users recognise and abide by the legal requirements associated with these rights.

Take down policy

The University of Edinburgh has made every reasonable effort to ensure that Edinburgh Research Explorer content complies with UK legislation. If you believe that the public display of this file breaches copyright please contact openaccess@ed.ac.uk providing details, and we will remove access to the work immediately and investigate your claim.



1 **Sestrins induce natural killer function in senescent-like CD8⁺ T cells**

2 Branca I. Pereira^{1†}, Roel P. H. De Maeyer^{1†}, Luciana P. Covre^{1,2†}, Djamel Nehar-Belaid^{3†},
3 Alessio Lanna^{1,4}, Sophie Ward⁵, Radu Marches³, Emma S. Chambers¹, Daniel C. O.
4 Gomes², Natalie E. Riddell^{1,6}, Mala K. Maini¹, Vitor H. Teixeira⁷, Samuel M. Janes⁷, Derek
5 W. Gilroy⁸, Anis Larbi⁹, Neil A. Mabbott¹⁰, Duygu Ucar³, George A. Kuchel¹¹, Sian M.
6 Henson¹², Jessica Strid⁵, Jun H. Lee¹³, Jacques Banchereau³, Arne N. Akbar^{1*}

7

8 **Affiliation:**

9 ¹ Division of Infection and Immunity, University College London, London, UK.

10 ² Núcleo de Doenças Infecciosas, Universidade Federal do Espírito Santo, Vitória, Brazil.

11 ³ The Jackson Laboratory for Genomic Medicine, Farmington, Connecticut, USA.

12 ⁴ Nuffield Department of Medicine, University of Oxford, Oxford, UK.

13 ⁵ Department of Medicine, Imperial College London, London, UK.

14 ⁶ Faculty of Health & Medical Sciences, University of Surrey, Guildford, UK.

15 ⁷ Lungs for Living Research Centre, UCL Respiratory, University College London, London
16 UK.

17 ⁸ Division of Medicine, University College London, London, UK.

18 ⁹ Singapore Immunology Network (SIgN), Agency for Science, Technology and Research
19 (A*STAR), Immunos Building, Biopolis, Singapore, Singapore.

20 ¹⁰ Roslin Institute and Royal (Dick) School of Veterinary Studies, University of Edinburgh,
21 Edinburgh, UK.

22 ¹¹ University of Connecticut Center on Aging, University of Connecticut, Farmington,
23 Connecticut, USA.

24 ¹² William Harvey Research Institute, Barts and The London School of Medicine and
25 Dentistry, Queen Mary University of London, London, UK.

26 ¹³ Department of Molecular & Integrative Physiology, University of Michigan, Ann Arbor,
27 Michigan, USA.

28

29 † These authors contributed equally.

30

31 ***Corresponding author:**

32 **Professor Arne N Akbar**

33 Division of Infection and Immunity, University College London,

34 Rayne Institute, 5 University Street, London, WC1E 6JF

35 Email: a.akbar@ucl.ac.uk

36 **Abstract**

37 Ageing is associated with re-modelling of the immune system to enable the maintenance of
38 life-long immunity. In the CD8⁺ T cell compartment, ageing results in the expansion of highly-
39 differentiated cells that exhibit characteristics of cellular senescence. Here we found that
40 CD27⁻CD28⁻CD8⁺ T lost the signalling activity of the T cell antigen receptor (TCR) and
41 expressed a protein complex containing the agonistic NK receptor NKG2D and the NK
42 adaptor molecule DAP12, which promoted cytotoxicity against cells that expressed NKG2D
43 ligands. Immunoprecipitation and imaging cytometry indicated that the NKG2D-DAP12
44 complex was associated with sestrin 2 (Sesn2). The genetic inhibition of Sesn2 resulted in
45 decreased expression of NKG2D and DAP12 and restored TCR signaling in senescent-like
46 CD27⁻CD28⁻CD8⁺ T cells. Therefore, during ageing, sestrins induces the reprogramming of
47 non-proliferative senescent-like CD27⁻CD28⁻CD8⁺ T cells to acquire a broad-spectrum,
48 innate-like killing activity.

49

50 Introduction

51 Immunity declines during ageing and this is associated an increased incidence of infections
52 and malignancy¹. It is therefore essential to understand mechanisms that contribute to
53 altered immunity in older individuals in order to identify possible therapeutic targets. Because
54 the thymus involutes from puberty onwards, its contribution to the maintenance of the T cell
55 pool decreases considerably during ageing. Instead, antigen specific T cells are maintained
56 in older individuals by repeated episodes of activation and proliferation triggered by specific
57 or cross-reactive antigenic challenge or by homeostatic cytokines². This extensive
58 proliferative activity leads ultimately to extreme functional differentiation and the
59 development of T cell senescence associated with telomere erosion, decreased signalling
60 through the T cell antigen receptor (TCR), activation of the telomere-extending enzyme
61 telomerase and also growth arrest³⁻⁵. Because the replicative activity of T cells is impaired as
62 senescence develops, mechanisms other than T cell proliferation may be required to
63 maintain optimal immune protection during ageing.

64 Highly-differentiated CD8⁺ T cells that lose expression of the surface receptors CD28 and
65 CD27 (CD27⁻CD28⁻) exhibit senescent-like characteristics that include low proliferative
66 activity, short telomeres, low telomerase activity and expression of senescence-associated
67 cell surface (CD57 and KLRG1) and intracellular (the MAP kinase p38, γH2AX) molecules⁴.
68 CD27⁻CD28⁻CD8⁺ T cells also upregulate receptors associated with natural killer (NK) cells,
69 such as inhibitory (KLRG1, NKG2A) and activatory proteins (NKG2C and NKG2D)⁶. Whether
70 the acquisition of the senescence-like characteristics and the expression of NK receptors
71 (NKR) are linked or are controlled independently remains unclear.

72 Sestrins are stress-sensing proteins, induced by conditions of low glucose or oxidative stress
73 or cellular senescence, that inhibit TCR activation and CD4⁺ T cell proliferation in both mice
74 and humans⁷. Here we showed that sestrins inhibited the expression of the TCR signaling
75 molecules LAT, ZAP70 and LCK in mouse and human CD8⁺ T cells, and concomitantly

induced the expression of both inhibitory and activating NKRs. Furthermore, sestrins regulated the association of NKG2D with the scaffold protein DAP12, which converts it into an activating receptor that can trigger the secretion of cytokines and cytotoxicity towards target cells bearing NKG2D ligands, independently of the TCR. Collectively, these data indicate that senescent-like CD8⁺ T cells are not a defective end-stage population. Instead these cells while non-proliferative, are instead re-programmed during differentiation to recognize and kill via both TCR⁸ as well as NKR recognition mechanisms, a process regulated by the sestrins. The repurposing of senescent-like CD8⁺ T cells to mediate innate-like functional activity may be crucial to mitigate against the increased burden of tumours and stromal senescent cells that accumulate in tissues during ageing^{9,10}.

86

87 **Results**

88 **Human CD8⁺ T_{EMRA} cells upregulate NKRs and adapters but decrease TCR** 89 **components**

First, we isolated peripheral blood CD8⁺ T cell subsets from six healthy donors and compared transcriptomes using Affymetrix U133 plus 2 microarrays of CD27⁺CD45RA⁻CD8⁺ central memory T (T_{CM}) cells, CD27⁻CD45RA⁻CD8⁺ effector memory T (T_{EM}) cells and CD27⁻CD45RA⁺CD8⁺ terminal effector memory T (T_{EMRA}) cells relative to the CD27⁺CD45RA⁺CD8⁺ naïve T (T_N) cells (**Fig. 1a** and **Extended Data Fig. 1a**). Differentially expressed genes in these CD8⁺ T cell subsets were identified based on a minimum of a 2-fold change ($p < 0.05$, false-discovery rate (FDR) for multiple comparisons $< 0.05\%$ (Supplementary table 1). Hierarchical clustering of genes associated with effector cell function indicated a transcriptional signature that distinguished T_{EMRA} cells from T_N cells (**Fig. 1b,c**). Genes involved in co-stimulation (*Cd28*, *Cd27*), TCR signaling (*Trac*, *Cd3e*, *Cd3g*, *Lck*, *Lat*, *Plcg1*) and proliferation and cell cycle control (*Ccne1*, *Ccnd3*) were downregulated in T_{EMRA} compared to T_N (**Fig. 1b,c**). Compared to CD8⁺ T_N cells, CD8⁺ T_{EMRA} cells upregulated genes

102 encoding the transcription factors *Zeb2* (fold change: 10.75, $p < 0.0001$) and *Zbtb16*
 103 (encoding PLZF, fold change: 6.48, $p < 0.0001$, **Fig. 1b**, Supplementary table 2) which are
 104 known to regulate terminal differentiation of memory T cells¹¹ and the development of innate-
 105 like features in T cells in mice^{12,13}. *Zbtb16* was also increased in T_{CM} and T_{EM} compared to T_N
 106 cells (7.7- and 4.8-fold respectively; Supplementary table 2). T_{EMRA} cells upregulated genes
 107 encoding NKRs (including *Kir* family members, *Nkg2a/c*, and *Klrg1*), innate signalling
 108 adaptors (*Tyrbp*, encoding DAP12) and molecules involved in cytotoxicity (*Gzma/b*, *Prf*,
 109 *Fasf*, *Itgav* and *Itgb1*)¹⁴. T_{EMRA} cells also upregulated chemokine receptors associated with
 110 the migration of NK cells into tissues (*Cx3cr1*, *S1pr5*, and *Cmklr1*)¹⁵, indicating that the
 111 differentiation of CD8⁺ T cells from T_N into T_{EMRA} was associated with a transcriptional
 112 program that promoted cytotoxic effector functions at the expense of proliferative potential
 113 and suggested that highly differentiated CD8⁺ T cells may express effector functions
 114 independent of the TCR.

115 Flow cytometric analysis indicated that the expression of NKRs (listed below) on non-NK
 116 cells was elevated on CD3⁺CD27⁻CD45RA⁺CD8⁺ T_{EMRA} cells (**Fig. 1d, Extended Data 1a**) in
 117 PBMCs isolated from a separate cohort of healthy donors (n = 22; median age = 52; range =
 118 25-83). The repertoire of NKRs expressed on CD8⁺ T_{EMRA} cells was diverse and included
 119 both activating (NKG2D, NKG2C and KIR2DS) and inhibitory (NKG2A, KIR2DL/KIR3DL and
 120 CD244) receptors, as well as the maturation markers KLRG1 and CD57 (**Fig. 1D, Extended**
 121 **Data 1b**). Expression of CD28 and CD27 is sequentially lost on CD8⁺ T cells as they
 122 transition from CD27⁺CD28⁺ CD8⁺ T_N cells to CD27⁺CD28⁻ intermediate CD8⁺ T cells and to
 123 terminal, or senescent-like, CD27⁻CD28⁻ CD8⁺ T cells^{16,17}. To analyse the expression of the
 124 TCR signalling machinery in CD8⁺ T_{EMRA} cells, we isolated CD8⁺ T cell subsets by their
 125 relative expression of CD27 and CD28, as the use of CD27 and CD28 as markers enabled
 126 the isolation of more cells for functional analyses. The CD27⁻CD28⁻CD8⁺ T cell subset
 127 contained the T_{EMRA} subset and T_{EM} (**Extended Data 1c**) and had increased expression of
 128 NKRs compared to CD27⁺CD28⁺CD8⁺ T_N cells (**Extended Data 2a**). Senescent-like CD8⁺ T

cells, either identified as CD27⁻CD28^{-18,19} or as CD27⁻CD45RA⁺²⁰ increase in both number and proportion during ageing and exhibit markers of senescence^{4,5,7,20}. Immunoblots showed a significant downregulation of LCK, LAT and PLCγ1, but upregulation of Zap70 in CD27⁻CD28⁻CD8⁺ T cells compared to CD8⁺ T_N cells (**Fig. 1e**). CD27⁻CD28⁻CD4⁺ T cells also acquired cell-surface expression of NKR (including KLRG1, NKG2C and NKG2D), but to a lower degree than CD27⁻CD28⁻CD8⁺ T cells (**Extended Data 2b**). Together, these findings indicate the increased expression of NKR on CD8⁺ T cells with characteristics of terminal differentiation and senescence.

Individual T_{EMRA} CD8⁺ T cells are senescent, and express NKR and cytotoxic machinery

To investigate whether the NKR, the cytotoxicity-related molecules and the senescence markers were expressed on individual CD8⁺ T_{EMRA} cells, we used single cell RNA-sequencing (scRNA-seq) to investigate the transcriptomes of ~62,000 CD8⁺ T cells isolated from six healthy old donors. CD8⁺IL-7R⁺ and CD8⁺IL-7R⁻ T cells were FAC-sorted from each donor resulting in 12 samples (**Extended data 3a**). Sorts yielded an average of 6199 CD8⁺IL-7R⁺ cells (SD 1582) and 4192 CD8⁺IL-7R⁻ cells (SD 1269) per donor, with an average of 1043 and 1011 genes per cell, respectively (**Extended data 3b,c**). After discarding hybrid transcriptomes (multiplets) using Scrublet (Methods), raw data from the 12 samples (six CD8⁺IL-7R⁺ and six CD8⁺IL-7R⁻ T cells) were combined. scRNA-seq profiles that passed the quality control (**Extended data 3d**) were then corrected for technical batch effects (e.g. 10x run) using BBKNN. Unbiased clustering followed by a two-dimensional uniform manifold approximation and projection (UMAP) on the corrected data identified 13 distinct clusters (**Fig. 2a**). Cluster assignments were independent of batch (**Extended data 3e**) and donor (**Extended data 3f**) effects. The CD8⁺IL-7R⁺ and CD8⁺IL-7R⁻ groups associated with distinct sets of clusters (**Fig. 2b**). The number of cells within each cluster varied from 9,263 to 915 (**Extended data 3g**) and their expression of *Il7r* mRNA was confirmed (**Extended data 4a**). We assigned clusters to cell types based on differential

analysis comparing expression values among cells from a given cluster to all other cells (Supplementary Table 3). All clusters expressed transcripts for *Cd3e* and *Cd8*, but not *Cd4* (**Fig. 2c**). We could identify clusters of T_N cells (expressing *Cd27*, *Ccr7*, *Sell* or *Cd28*) and effector T cells (expressing *Klrg1*, *Prf1* or *Gzmb*) (**Fig. 2c**). Based on this expression profile, clusters C0, C4 and C8 were defined as CD8⁺ T_N cells, and C1, C2 and C6 as CD8⁺ T_{EMRA} cells (**Fig. 3a**). A second round of clustering performed on these six clusters confirmed the distinct transcriptomic profiles of the CD8⁺ T_N and CD8⁺ T_{EMRA} compartments (**Fig. 3b**, **Extended data 4b**) and confirmed the enrichment of the CD8⁺ T_{EMRA} compartment within the CD8⁺IL-7R⁻ cells (**Extended data 4c**). CD8⁺ T_N cells were characterized by the expression of *Cd27*, *Cd28*, *Ccr7* and *Sell*, while CD8⁺ T_{EMRA} cells showed an upregulation of *Klrg1*, *Prf1* or *Gzmb* relative to the clusters of CD8⁺ T_N cells (**Extended data 4d**).

The expression of 15 NK-associated genes, including *Fcgr3a* (encoding the Fcγ receptor CD16), the NK-related receptors *Fcrl6*, *Klrc1* and *-2*, *Klrg1*, and *Tyrobp* (**Fig. 3c**) was used to define an “NK score”. This confirmed that CD8⁺ T_{EMRA} cells become NK-like compared to CD8⁺ T_N cells (**Fig. 3d**; Supplementary table 4). Similarly, we used expression of senescence-related genes, such as *B3gat1* (encoding the enzyme that creates the CD57 epitope), the cell cycle regulators *Cdkn1a* and *Cdkn2a*, and sMAC components such as *Sesn2* and *Mapk1* to create a “senescence score” to determine that CD8⁺ T_{EMRA} are senescent compared to CD8⁺ T_N cells (**Fig. 3e,f**, Supplementary table 4). Although expression of LCK, PLC-γ1 and LAT proteins was decreased in CD27⁻CD28⁻CD8⁺ T cells compared to T_N CD8⁺ cells (**Fig. 1e**), the mRNA for these TCR signalling components was similar in T_{EMRA} and T_N CD8⁺ cells analysed by scRNA-seq (not shown), suggesting their expression might be regulated by post-translational modification in CD27⁻CD28⁻CD8⁺ T cells. These observations suggested that T_{EMRA} CD8⁺ T cells had characteristics of cellular senescence and expressed a range of NKRs, NK adaptors and cytotoxic mediators.

NKG2D and DAP12 induce cytotoxicity in senescent T cells

We next investigated whether CD27⁺CD28⁺CD8⁺ T cells had NK cell-like functions independently of TCR-MHC interactions. Based on the expression of the degranulation marker CD107a²¹, CD27⁺CD28⁺CD8⁺ T cells killed K562 cells, an MHC class I-deficient tumour cell line, with the same efficiency as NK cells (**Fig. 4a**). These data were confirmed using a calcein-release assay (**Extended data 5a,b**). To address whether NKG2D mediated the cytotoxic activity of CD27⁺CD28⁺CD8⁺ T cells, we knocked down NKG2D in CD28⁺CD8⁺ T cells with a small interfering RNA (siRNA) specific for NKG2D (siNKG2D CD8⁺T cells) and assessed their ability to kill MHC class I-deficient C1R cells transfected with the NKG2D ligand MICA*008 (C1R-MICA cells) when co-cultured for 6 hours (**Extended data 5c,d**). CD28⁺CD8⁺T cells transfected with scrambled siRNA (siCtrl) showed increased degranulation, measured by CD107a exposure, towards C1R-MICA compared to C1R cells, while the cytotoxicity of siNKG2D CD8⁺ T cells towards the C1R-MICA cells was inhibited compared to siCtrl (**Fig. 4b**), indicating that CD28⁺CD8⁺ T cells could kill target cells in a manner dependent on NKG2D.

Expression of NKG2D on the cell surface requires its association with adaptor proteins that stabilise the immunoreceptor complex and provide it with signalling activity²². NKG2D associates with the adaptor molecules DAP10 and DAP12. DAP10 contains an YxxM-motif that activates PI3K^{23,24}, while DAP12 has an ITAM-motif that can recruit and activate ZAP70-Syk triggering cytokine release and cytotoxicity²⁵⁻²⁷. In human CD8⁺ T cells, NKG2D is predominantly associated with DAP10^{23,27} (**Extended data 5e**), which allows it to act as a co-stimulatory signal for the TCR. Immunoblot analysis (**Fig. 4c**) and intracellular flow cytometry (**Fig. 4d**) indicated increased expression of DAP12 in CD27⁺CD28⁺CD8⁺ T cells compared to T_N CD8⁺ cells, corresponding to the transcriptomic data indicating that *Tyrobp* (which encodes DAP12) was strongly induced in T_{EMRA} CD8⁺ T cells compared to T_N CD8⁺ cells (**Fig. 1c, 3c**). To investigate whether the killing activity of CD27⁺CD28⁺CD8⁺ T cells was mediated by DAP12 association with NKG2D we immunoprecipitated NKG2D from

CD28⁺CD8⁺ or CD28⁻CD8⁺ T cells isolated from peripheral blood of healthy donors. DAP12 associated with NKG2D only in the CD28⁻CD8⁺ T cells (**Fig. 4e**).

We next investigated whether ligation of NKG2D induced the phosphorylation of ZAP70-Syk in CD27⁻CD28⁻CD8⁺ T cells. CD3 ligation with an anti-CD3 monoclonal antibody (mAb) induced the phosphorylation of ZAP70-Syk, as expected, while using an anti-NKG2D mAb alone induced more p-ZAP70 and p-Syk compared to anti-CD3 alone (**Fig. 4f**), indicating that CD27⁻CD28⁻CD8⁺ T cells can be activated by both the TCR and NKG2D, but show an increased propensity to respond to the latter. Anti-NKG2D stimulation alone was sufficient to induce expression of granzyme B and secretion of IFN- γ in CD27⁻CD28⁻CD8⁺ T cells (**Fig. 4g**). siRNA-mediated silencing of DAP12 in CD28⁻CD8⁺ T cells impaired the cytolytic degranulation of CD28⁻CD8⁺ T cells towards C1R-MICA cells compared to scrambled siRNA control-transfected CD28⁻CD8⁺ T cells (**Fig. 4h**). Thus, DAP12 expression was upregulated in CD28⁻CD8⁺ T cells and was necessary and sufficient to mediate NKG2D-dependent cytotoxicity.

Sestrins block TCR signalling but increase NKR in CD8⁺ T cells

CD27⁻CD28⁻CD8⁺ T cells have reduced proliferative activity after TCR stimulation^{4,5,7}. We investigated whether reduced expression of the components of the CD3-TCR complex compromised the efficiency of proximal TCR signaling. Phospho-flow cytometry indicated impaired phosphorylation of CD3 ζ after stimulation with CD3 antibodies in CD27⁻CD28⁻CD8⁺ compared to CD27⁺CD28⁺CD8⁺ T cells (**Fig. 5a**). Although the expression of total Zap70 was increased in CD28⁻CD27⁻CD8⁺ T cells (**Fig. 1e**), its phosphorylation was impaired in these cells compared to CD28⁺CD27⁺CD8⁺ T cells following CD3 activation (**Fig. 5b**).

The stress-sensing proteins sestrins induce characteristics of senescence in CD4⁺ T cell by forming a complex with the kinase AMPK and the MAP kinases that is inhibitory for signalling through the TCR⁷. Flow cytometry (**Fig. 5c,d**) and immunoblotting (**Fig. 5e**) indicated that peripheral blood CD27⁻CD28⁻CD8⁺ T cells exhibited increased expression of sestrin 1 and

sestrin 2 compared to CD27⁺CD28⁺CD8⁺ T cells. Sestrin 2 was upregulated in total CD8⁺ T cells from donors older than 65 years compared to those between 18-35 years (**Extended data 5f**). In addition, CD27⁻CD28⁻CD8⁺ T cells had increased amounts of activated Jnk MAP kinase (P-Jnk) compared to CD27⁺CD28⁺CD8⁺ T cells (**Fig. 5e**). Immunoprecipitation experiments indicated that DAP12, sestrin 2 and Jnk were associated with NKG2D in CD27⁻CD28⁻CD8⁺ T cells (**Fig. 6a**), while imaging cytometry indicated that sestrin 2, DAP12 and p-Jnk co-localised in CD27⁻CD28⁻CD8⁺ but not CD8⁺ T_N cells (**Fig. 6b,c**). These observations suggested that sestrin 2 associated with NKG2D-DAP12-Jnk in CD27⁻CD28⁻CD8⁺ cells.

Next, we tested whether sestrins regulated the expression of NKG2D in human CD28⁻CD8⁺ T cells. Peripheral blood CD28⁻CD8⁺ T cells isolated from healthy donors were lentivirally transduced with shRNA against Sesn1, 2 and 3 (shSesn) had significantly reduced expression of DAP12 (**Fig. 6d**) and NKG2D compared to CD28⁻CD8⁺ T cells transduced with control vectors (**Fig. 6e**), indicating sestrins modulated the expression of NKG2D in these cells. siRNA-mediated (**Fig. 6f**) or inhibition of Jnk with the small molecule inhibitor SP-600125 (**Fig. 6g**) also reduced the expression of NKG2D, while increasing the frequency of CD28 expression and restoring proximal TCR signalling following anti-CD3 mAb ligation in CD28⁻CD8⁺ T cells compared to untreated controls (**Fig. 6f,g**). This indicated a reconstitution of T cell related functions, implying sestrins may act through Jnk to induce expression of NKG2D expression in CD28⁻CD8⁺ T cells.

YFV induces the upregulation of NKR on CD8⁺ T cells

Next we tested if the upregulation of NKRs by CD8⁺ T cells occurred exclusively as a result of cellular senescence or if NKRs were expressed on less-differentiated subsets of CD8⁺ T cells in response to antigenic stimulation and the expression was maintained as cells differentiated towards senescence. Using publicly available RNA-seq gene expression data generated in a cohort of 12 individuals vaccinated against yellow fever²⁸. We compared T_E

CD8⁺ T cells, defined as YFV-tet⁺ cells at day 14 post-vaccine, and CD8⁺ T_M cells, defined as YFV-tet⁺ cells 4-13 years post-vaccine and these populations were compared to YFV-tet⁺ CD8⁺ T_N cells. Cytotoxic mediators such as *Fasl*, *Prf1*, *Gzma* and *Gzmb* were highly expressed in T_E and T_M compared to T_N CD8⁺ T cells (**Extended data 6**). Additionally, there was a significant upregulation of multiple NKRs, including many of the *Kir*, *Fcgr3a*, *Cd57* and *Klrc1* on T_E and T_M compared to T_N CD8⁺ T cells, as well as chemokine receptors (*S1pr5*, *Cmklr1* and *Cx3cr1*) and NK adaptor proteins such as *Tyrbp* (**Extended data 6**). The upregulation of these molecules occurred on YFV-tet⁺ T_E CD8⁺ T cells during the effector phase of the response and was maintained in long-lived YFV-tet⁺ T_M (**Extended data 6**). Based on published data, YFV-tet⁺ T_M cells lack markers of senescence like CD57, are CD27⁺CD28⁺ and are polyfunctional with regard to cytokine secretion²⁹. Unlike the CD8⁺ T_{EMRA} cells, YFV-tet⁺ CD8⁺ T_M cells exhibit proliferative potential *in vitro*, suggesting that they were not terminally differentiated²⁹. YFV-tet⁺ T_E and T_M CD8⁺ T cells showed slight downregulation of the TCR signalosome (*Lat*, *Plcg1*, *Zap70*) compared to T_N cells (**Extended data 6**). Of note, sestrin 2 was upregulated in the YFV-tet⁺ T_E and T_M compared to T_N CD8⁺ T cells (**Extended data 6**). This analysis indicated that the expression of NKR on CD8⁺ T cells was not limited to senescent CD27⁻CD28⁻CD8 T cells but was also a feature of YFV-tet⁺ T_E and T_M CD8⁺ T cells after activation *in vivo*.

Sestrins regulate the function of CD8⁺ T cells *in vivo*

Sestrins regulate the decreased function of CD4⁺ T cells in aged mice and humans⁷. We next investigated if sestrins directly regulated the expression of NKRs in CD8⁺ T cells in young (~6 weeks) and old (~18 months) wild-type mice and old (~18 months) *Sesn1*^{-/-} and *Sesn2*^{-/-} mice. Mice were vaccinated subcutaneously against methylated BSA (mBSA) and re-challenged with mBSA in the footpad two weeks later to induce a delayed-type hypersensitivity (DTH) response as an index of successful immune induction. All mice

286 mounted a DTH response to the re-challenge, but the DTH response in old wild-type, *Sesn1*^{-/-}
 287 ^{-/-} and *Sesn2*^{-/-} mice resulted in increased footpad swelling compared to young wild-type mice
 288 (**Fig. 7a**). The response resolved more slowly in old wild-type compared to young wild-type
 289 mice, while old *Sesn1*^{-/-} and *Sesn2*^{-/-} mice resolved faster than old wild-type mice (**Fig. 7a,b**).
 290 Spleen weights were equivalent in all groups post-mBSA challenge (**Extended data 7a**).
 291 There were no changes in the proportions of splenic NK cells, iNKT cells, CD4⁺ T cells and
 292 CD8⁺ T cells in all old and young mice following the DTH response (**Extended data 7b,c**).
 293 However, CD44⁺CD62L⁻CD8⁺ T_{EFF} cells expanded, while CD44⁻CD62L⁺CD8⁺ T_N cells
 294 decreased in old wild-type mice, but not in old *Sesn1*^{-/-} and *Sesn2*^{-/-} mice, compared to
 295 young wild-type mice (**Extended data 7d,e**).

296 Expression of NKG2D and DAP12, as well as NKG2A, NKG2C, NKG2E and Ly49 was
 297 higher on the CD8⁺ T cells from the old wild-type mice compared to the young wild-type
 298 mice, whereas their expression was lower in both old *Sesn1*^{-/-} and *Sesn2*^{-/-} mice compared to
 299 old wild-type mice (**Fig. 7c-e and Extended data Fig. 7f**), suggesting the expression of
 300 these receptors was modulated by sestrins. Importantly, the expression of NKG2D, as well
 301 as NKG2A, NKG2C, NKG2E on CD3⁺TCRβ⁻NK1.1⁺ NK cells or TCRβ⁺CD1d-tet⁺ iNKT cells
 302 was similar in young wild-type, old wild-type and both *Sesn1*^{-/-} and *Sesn2*^{-/-} mice (**Fig. 7f,g**),
 303 indicating that sestrins uniquely regulated the expression of NKRs in CD8⁺ T cells. To
 304 examine the effect of sestrin deficiency on the cytotoxic function of CD8⁺ T cells *in vivo*, 24-
 305 month old wild-type mice and 24-month old *Sesn1*^{-/-}*Sesn2*^{-/-}*Sesn3*^{+/-} mice were NK-depleted
 306 with intra-peritoneal anti-NK1.1 treatment prior to intra-venous injection of equal numbers of
 307 5tgm1 myeloma cells expressing Rae-1, the mouse equivalent of MICA/B, and Rae-1⁻
 308 splenocytes. Six hours post-transfer of target cells, more Rae-1⁺ 5TGM1 cells were detected
 309 in the spleens of *Sesn1*^{-/-}*Sesn2*^{-/-}*Sesn3*^{+/-} mice compared to wild-type mice (**Fig. 7h**). This
 310 resulted from decreased specific lysis of Rae-1⁺ 5TGM1 target cells in *Sesn1*^{-/-}*Sesn2*^{-/-}
 311 *Sesn3*^{+/-} mice compared to wild-type mice (**Fig. 7i**). These observations indicated that the

sestrins regulated the expression of NKG2D and DAP12 and confer NK cell-like cytotoxic activity to CD8⁺ T cells of old animals *in vivo*.

Discussion

Here we provide phenotypic, functional and mechanistic data to support the idea that as CD8⁺ T cells differentiated towards senescence they lose the expression of co-stimulatory molecules e.g. CD28 and CD27 and they downregulate TCR signalling molecules such as Lck and LAT concomitantly with upregulating the expression of NKR such as NKG2D, NKG2A and CD16. The CD28⁻CD27⁻ CD8⁺ T cells also acquire a senescent phenotype compared to CD28⁺ CD27⁺CD8⁺ T cells. This transition for TCR to NKR expression during CD8⁺ T cell differentiation was associated with the acquisition of the ability to kill tumour cells both *in vitro* and *in vivo* by an NKR dependent process. Furthermore, the switch between TCR and NKR expression was regulated by the sestrins.

Other studies indicate that altered TCR signalling pathways are associated with the development of unconventional functions that are not restricted to the TCR-MHC interactions^{30,31}. The suppression of TCR signalling along with an acquired responsiveness to innate stimuli was proposed to be a characteristic that defines innate-like T cells³². We found that the TCR to NKR switch was dependent on the kinase Jnk in CD8⁺ and CD4⁺ T cells⁷, but the mechanism by which sestrins modulate this transition remains unclear. Experiments in sestrin-deficient mice indicated that these molecules did not regulate the expression of NKRs in NK cells or iNKT cells and it remains unclear if sestrins may regulate the function of other types of innate-like T cells e.g. $\gamma\delta$ T cells.

This reprogramming of senescent CD8⁺ T cells would repurpose them to exhibit broad NK-like activity. This could be particularly relevant for T cells specific for persistent pathogens,

such as cytomegalovirus (CMV) and Epstein-Barr virus (EBV) that accumulate during ageing³³⁻³⁵. Our data suggest that in addition to their role in maintaining long-term specific immunity against these viruses, these cells may also recognize a cells infected by different viruses and also tumour cells via an NK-like function, in an antigen-independent manner thus enabling them to exhibit broad protective function.

While the long-term blockade of sestrins may be dangerous, as it would enhance the proliferation of senescent-like T cells that harbour DNA damage, temporary blockade could be exploited to increase the number of antigen-specific T cell numbers to boost vaccine responsiveness in aged individuals⁷. In this context, it is important to know when the expression of sestrins and NKR occurs on T cells after vaccination. Gene expression studies in YFV-specific CD8⁺ T cells after vaccination of previously non-immunized individuals found that both NKR and sestrin expression were upregulated in the effector phase of the response (weeks) and maintained in the T_M cells for years^{28,29}. This indicates that sestrins are induced in effector and memory CD8⁺ T cells during primary vaccination responses and not only on senescent CD8⁺ T cells. It would be important to determine how these molecules are expressed during a secondary response and during vaccination of older humans.

These findings raise questions about the biological significance of such changes and the possible advantage of generating T cells with NK cell-like characteristics. The accumulation of T_{EMRA} CD8⁺ T cells was reported to be a predictor of successful ageing⁸. One reason for this may be the acquisition of NKR by T_{EMRA} CD8⁺ T cells may allow them to broaden their capacity for immune surveillance by utilising different recognition systems, which may compensate in part for decreased output of T_N in older subjects³⁶. Given the increased burden of tumours and infections with age, the expansion of NK-like CD8⁺ T cells would be

an advantageous adaptation that enable the recognition of many different tumour cell types. Furthermore, non-lymphoid senescent cells are pro-inflammatory and increase in number in many organs during ageing^{37,38}. The removal of these senescent cells from tissues has been shown to enhance organ function and retard age-related functional decline^{39,40}. Since NK and CD8⁺ T cells can also recognize and kill senescent cells via NKG2D mediated mechanisms^{9, 10,41} another role of NKR expressing senescent CD8⁺ T cells may be to participate in the surveillance and elimination of senescent tissue cells *in vivo*. This study highlights the central role of the sestrins in functional fate decisions in T cells. It will be important to identify if these molecules also have similar roles in other cell types.

Acknowledgements

We thank A. Toubert from INSERM U.1160 and laboratoire d'Immunologie et d'Histocompatibilité, Hôpital Saint-Louis, Université Paris Diderot, Sorbonne Paris Cité for the kind gift of the C1R-MICA cell line. B.I.P. was supported by the Portuguese Foundation for Science and Technology and Gulbenkian Institute for Science sponsoring the Advanced Medical Program for Physicians (PFMA). This work was supported by the Medical Research Council (grant MR/P00184X/1 to A.N.A), the Ministry of Education of Brazil (Grant BEX9414/14-2 to L.P.C.), the Wellcome Trust (Grant AZR00630 to A.L.), UCL Business to S.M.H and A.N.A (for the microarray work), the National Institutes of Health (R01DK102850 and R01DK111465 to J.H.L.), the NIH/NIAID (R01 AG052608 and R01 AI142086) to JB and the Biotechnology and Biological Science Research Council (Grant BB/L005336/1 to N.E.R.). R.P.H.D was supported, in part, by the NIHR UCLH Biomedical Research Centre, S.M.H. is funded by the Springboard award from the Academy of Medical Science and the Wellcome Trust. A.L. is a Sir Henry Wellcome Trust Fellow sponsored by Prof. Michael L. Dustin (University of Oxford). S.M.J. is a Wellcome Trust Senior Fellow in Clinical Science and is supported by the Rosetrees Trust, the Welton Trust, the Garfield Weston Trust and UCLH Charitable Foundation. S.M.J. and V.H.T. have been funded by the Roy Castle Lung Cancer Foundation. DU is supported by National Institute of General Medical Sciences

(NIGMS) under award number GM124922. GAK is supported by the Travelers Chair in Geriatrics and Gerontology, as well as National Institute on Aging (AG061456; AG048023; AG063528; AG060746; AG021600; AG052608; AG051647).

Author contributions: B.I.P., L.P.C and R.P.H.D. designed and performed the experiments, analysed the data and wrote the manuscript. DNB designed and analysed the single cell RNA-seq data under the supervision of JB and DU. RM performed all the experiments with the healthy older adult subjects. GAK recruited all the healthy older adult donors subjects in Farmington. CT. A.L., E.S.C. and N.E.R. designed and performed experiments. S.W. and J.S. designed and performed *in vivo* cytotoxicity studies. S.M.H. and A.N.A. designed and performed the microarray studies. N.A.M., V.H.T. and S.M.J. analysed the microarray and RNA-seq data. D.C.O.G., D.W.G., J.H.L. and M.K.M. facilitated mouse experiments. D.E. designed and provided the lentiviral vectors. A.N.A. designed the experiments and reviewed and edited the manuscript and organized the collaborative infrastructure.

Competing interests: The authors have declared that no conflict of interest exists.

Materials and Methods

Study design

The study protocol was approved by the Ethical Committee of the Royal Free and University College London Medical School (Research Ethics number: 11/0473). Written informed consent was obtained from all study participants. Donors did not have any co-morbidity, were not on any immunosuppressive drugs, and retained physical mobility and lifestyle independence. For analyses involving the CD8⁺ T cell, IL-7R⁺/IL-7R⁻ single cell dataset studies were conducted following approval by the Institutional Review Board (IRB) of the University of Connecticut Health Center (IRB 14-194J-3). After receiving informed consent,

blood samples were obtained from 6 healthy old (>65 year old) research volunteers residing in the Greater Hartford, CT, region using services of the University of Connecticut Center on Aging Recruitment and Community Outreach Research Core and following previously published screening criteria (PMID:28904110).

Cell isolation and transfection

Peripheral blood mononuclear cells (PBMC) were isolated by density gradient (Ficoll–Hypaque, Amersham Biosciences, UK) from heparinized blood of healthy donors (n = 22, 26-83 years). Untouched NK and CD8⁺ T cells were freshly isolated by magnetic activated cell sorting (MACS, Miltenyi Biotec, UK) using a negative selection procedure. For microarray analysis, high-purity CD8⁺ T cell subsets were sorted on the basis of CD27 and CD45RA expression⁴², using a FACS Aria (BD Biosciences, UK) flow cytometer. For functional assays, CD8⁺ T cell subsets were freshly isolated according to CD27/CD28 expression by magnetic activated cell sorting (MACS, Miltenyi Biotec, UK), which identified analogous subsets but provided higher yields of viable cells (> 95% purity) as previously described^{5,7}. Double negative cells were obtained by complete negative isolation. We found that <1% of cells within these isolated populations expressed iNKT markers. Mucosal associated invariant T cells (MAIT) cells express TCR Va7.2 and these cells constitute ~5% of the peripheral CD8⁺ T cells pool in humans⁴³. We found 4% (range 1-7.5%) of these cells in isolated CD28⁺ CD27⁺, 3% (range 1-6.4) in the isolated CD28⁺ CD28⁺ and 2.9% (range 1-4.9%) in the isolated CD28⁺ CD27⁺ CD8⁺ T cells populations. The results obtained are therefore unlikely to be due to contaminating iNKT or MAIT cells in our CD8⁺ T cells populations.

Where indicated, freshly purified human CD8⁺ T cells were transfected with small interfering RNA (siRNA) for NKG2D (Santa Cruz Biotechnology, sc-42948) or DAP12 (sc-35172) by electroporation using the Amaxa Human NK Cell Nucleofector Kit and Nucleofector

technology (Lonza), according to the manufacturer's instructions. A scrambled control siRNA (sc-37007; Santa Cruz) was used throughout. Efficiency of siRNA transfection was confirmed by measuring the expression of the protein of interest using flow cytometry, 36-48 hours after transfection.

Microarray data acquisition

Cells purified by FACS were stimulated for 2 hours with 0.5 µg/ml plate-coated anti-CD3 (OKT3) and 5 ng/ml rhIL-2 before RNA isolation using the ARCTURUS PicoPure Isolation Kit (ThermoFisher). The concentration of small quantities of RNA was determined using Nanodrop. Linear amplification of 10 ng of total RNA was performed using the Ovation Biotin RNA amplification and labelling system (NuGEN). Fragmented, labelled cDNA was hybridized to Affymetrix U133 plus 2 arrays.

Single cell RNA sequencing

Sample processing: all samples were processed within one hour from venipuncture.

Cell Sorting: PBMCs were isolated from fresh whole blood using Ficoll-Paque Plus (GE) density gradient centrifugation. For cell sorting, we used fluorochrome-labeled antibodies specific for CD3 (UCHT1), CD27 (M-T271) (Biolegend), CD4 (RPA-T4), CD19 (HIB19), IgD (IA6-2), CD127 (HIL-7R-M21) (BD Biosciences), and CD8 (SCF121Thy2D3) (Beckman-Coulter). CD8⁺IL7R⁺ (CD8⁺CD127⁺) and CD8⁺IL7R⁻ (CD8⁺CD127⁻) T cells were sorted from the CD19⁻CD3⁺CD4⁻ fraction. Cell sorting was performed using FACS Aria Fusion (BD).

Blood preparation for single cell RNA sequencing (scRNA-seq): PBMCs were thawed quickly at 37°C and transferred to DMEM supplemented with 10% FBS. Cells were spun down at 400 g, for 10 min. Cells were washed once with 1 x PBS supplemented with 0.04% BSA and finally re-suspended in 1 x PBS with 0.04% BSA. Viability was determined using trypan blue staining and measured on a Countess FLII and samples with <80% viability were discarded. 12,000 cells were loaded for capture onto the Chromium System using the v2 single cell reagent kit (10X Genomics). Following capture and lysis, cDNA was synthesized

470 and amplified (12 cycles) as per manufacturer's protocol (10X Genomics). The amplified
471 cDNA was used to construct an Illumina sequencing library and sequenced on a single lane
472 of a HiSeq 4000.

473 **Single cell Raw data processing and data combination:** Illumina basecall files (*.bcl)
474 were converted to fastqs using cellranger v2.1.0, which uses bcl2fastq v2.17.1.14. FASTQ
475 files were then aligned to hg19 genome and transcriptome using the cellranger v2.1.0
476 pipeline, which generates a gene - cell expression matrix. The samples were merged
477 together using cellranger aggr from cellranger, which aggregates outputs from multiple runs,
478 normalizing them to the same sequencing depth (normalize=mapped) and then re-
479 computing the gene-barcode matrices and analysis on the combined data (See scripts here:
480 <https://github.com/dnehar/Temra-IL7R-Senescence>).

481 **Scrublet for multiplet prediction and removal:** Generally, we expected about 2 to 8% of
482 the cells to be hybrid transcriptomes or multiplets, occurring when two or more cells are
483 captured within the same microfluidic droplet and are tagged with the same barcode. Such
484 artifactual multiplets can confound downstream analyses. We applied Scrublet⁴⁴ python
485 package to remove the putative multiplets. Scrublet assigns each measured transcriptome a
486 'multiplet score', which indicates the probability of being a hybrid transcriptome. Multiplet
487 scores were determined for each individual (using the raw data), and 0.7% - 10.7% highest
488 scoring cells were tagged as multiplets after visual inspection of doublet score distributions
489 and excluded from the further analysis.

490 **Single cell processing, clustering and cell type classification:** The aggregated matrices
491 were fed into the Python-based ScanPy⁴⁵ workflow
492 (<https://scanpy.readthedocs.io/en/stable/>), which includes preprocessing, visualization,
493 clustering and differential expression testing. The pipeline we used was inspired by The
494 Seurat⁴⁶ R package workflow.

495 **Quality control and cell-filtering:** We applied the following filtering parameters: (i) all
496 genes that were not detected in ≥ 3 cells were discarded, (ii) cells with less than 400 total
497 unique transcripts were removed prior to downstream analysis, (iii) cells in which $> 20\%$ of
498 the transcripts mapped to the mitochondrial genes were filtered out, as this can be a marker
499 of poor-quality cells and (iv) cells displaying a unique gene counts $> 2,500$ genes were
500 considered outliers and discarded.

501 **Data normalization:** After discarding unwanted cells from the dataset, we normalized the
502 data. Library-size normalization was performed based on gene expression for each barcode
503 by scaling the total number of transcripts per cell to 10,000. We log-transformed the data
504 and then regressed out using the total number of genes and the fraction of mitochondrial
505 transcript content per cell. 1202 highly variable genes (HVG) were identified using
506 `filter_genes_dispersion` scanpy function and used to perform the principal component
507 analysis (PCA).

508 **Linear dimensional reduction using PCA and graph-based clustering:** Dimensionality
509 reduction was carried out in SCANPY via principal component analysis followed by Louvain
510 clustering UMAP visualization using the top 40 significant components (PCs)⁴⁷.

511 **Finding marker genes/evaluation of cluster identity:** To annotate the cell type of each
512 single cell transcriptome, we used both differential expression analysis between clusters and
513 classification based on putative marker gene expression. We applied the
514 '`tl.rank_genes_groups`' scanpy function to perform differential analyses, comparing each
515 cluster to the rest of the cell using Wilcoxon test (Supplementary Table 3). We only
516 considerate clusters that showed a distinct transcriptomic programs.

517 **Batch effect correction:** We performed a batch (10X genomics batch) correction using
518 BBKNN (<https://github.com/Teichlab/bbknn>)⁴⁸. More details about the parameters used can
519 be found as a Jupyter notebook here: <https://github.com/dnehar/Temra-IL7R-Senescence>.

520 **NK and Senescence scores:**

Gene lists (Table S3) were used to score NK or senescence expression in naïve and Temras CD8 T cells. To do so, we calculated the mean expression for each cell, within each cluster using the h5ad object (adata), as follow:

```
adata.obs['NK_score'] = adata.X[:,NK_markers].mean(1).
```

The scores were then plotted, as shown in Fig .3D.

Lentiviral transduction

Sestrin knockdown in human CD8⁺ T cells was achieved using a lentiviral transduction system as described previously⁹.

The pHIV1-SIREN-GFP system used for knockdown of gene expression possesses a U6-shRNA cassette to drive shRNA expression and a GFP reporter gene that is controlled by a PGK promoter⁵. The following siRNA sequences were used for gene knockdowns: CCTAAGGTTAAGTCGCCCTCG (shCTRL), CCAGGACCAATGGTAGACAAA (shSesn1), CCGAAGAATGTACAACCTCTT (shSesn2) and CAGTTCTCTAGTGTCAAAGTT (shSesn3). VSV-g pseudotyped lentiviral particles were produced, concentrated and titrated in HEK293 cells as described⁹.

Cells were cultured in RPMI-1640 medium supplemented with 10% heat-inactivated FCS, 100 U/ml penicillin, 100 mg/ml streptomycin, 50 µg/ml gentamicin, 2 mM L-glutamine (all from Invitrogen) and 0.5 ng/ml anti-mycoplasma (Bio-Rad) at 37 °C in a humidified 5% CO₂ incubator. Purified human highly differentiated CD28⁻CD8⁺ T cells were activated in the presence of plate-bound anti-CD3 (purified OKT3, 0.5 µg/ml) plus rhIL-2 (R&D Systems, 10 ng/ml), and then transduced with pHIV1-Siren lentiviral particles (multiplicity of infection (MOI) = 10) 72 h after activation.

Flow cytometry and Phospho-flow

Multi-parameter flow cytometry was used for phenotypic and functional analyses of PBMC. For analysis of surface markers, staining was performed at 4°C for 30 min in the presence of saturating concentrations of antibodies (listed in Supplementary table 5) and a live/dead

fixable Near-Infrared stain (Thermo Scientific, L10119). For intracellular analysis of cytokine secretion, cytotoxic granule expression, and sestrin 1, sestrin 2, DAP12, and DAP10 expression, cells were fixed and permeabilized with the Fix & Perm® Kit (Invitrogen, Life Technologies, UK), before incubation with indicated antibodies or the respective isotype controls. For imaging cytometry, samples were acquired on an Amnis ImageStreamX Mk2 using INSPIRE software, magnification 60X. Data were analysed using IDEAS v6.2 software (Amnis). Co-localization of signals was determined on a single cell basis using bright detail similarity (BDS) score analysis. Co-localization was considered with $BDS \geq 2.0$.

For Phospho-Flow cytometry, after staining for surface markers, CD8⁺ T cells were stimulated with anti-CD3 (purified OKT3, 10 µg/mL) for 30 minutes on ice, followed by crosslinking with goat anti-mouse IgG antibody during 30 minutes on ice. Cells were then transferred to an incubator at 37°C, and stimulation was terminated after 10 minutes, with immediate fixation with Cytofix Buffer (PBS containing 4% paraformaldehyde, BD Biosciences) followed by permeabilization with ice-cold Perm Buffer III (PBS containing 90% methanol, BD Biosciences) and staining with antibodies for phospho-proteins (listed in **Table 2**) for 30 minutes at room temperature. Samples were acquired on a LSR II flow cytometer (BD Biosciences) and analysed using FlowJo software (TreeStar).

Cytotoxic assays - CD107a degranulation assay

Freshly isolated NK and CD8⁺ T cell subsets were incubated at 37°C for 6 h with K562 or C1R-MICA/C1R cells, at a fixed effector to target (E:T) ratio of 2:1, in the presence of APC-conjugated CD107a antibody (BD Biosciences), as previously described⁶⁸. Brefeldin A (1µg/ml; Sigma-Aldrich) and Monensin (1 µg/ml; Sigma-Aldrich) were added in the final 5h-incubation period. Effector cells incubated alone in the presence phorbol-12-myristate-13-acetate (PMA, 50 ng/ml, Sigma-Aldrich) with ionomycin, (250 ng/ml, Sigma-Aldrich) were used as positive control whereas medium alone served as unstimulated (US) control. After incubation, cells were stained for surface markers for 30 min on ice, followed by intracellular

573 detection of cytokines (TNF- α and IFN- γ) and CD107a expression and analysed by flow
574 cytometry.

575 ***Cell lines***

576 K562 (human erythroleukemic) cell line was purchased from the European Collection of Cell
577 cultures (ECCAC, UK) and cultured in 25 cm² flasks (Nunc) in complete RPMI-1640. B-
578 lymphoblastoid cell lines, C1R and C1R transfected with MICA*008 (C1RMICA) were kindly
579 provided by Professor Antoine Toubert (INSERM UMR1160, Paris) and maintained in
580 complete RPMI-1640 in the presence of the aminoglycoside antibiotic G-418 (Sigma,
581 G8168) for selection of transfected cells⁴⁹.

582 ***Immunoblotting***

583 Human CD8⁺ T cell subsets purified using immunomagnetic separation (MACS) according to
584 CD27/CD28 expression were stimulated with anti-CD3 (purified OKT3, 10 μ g/mL) or anti-
585 NKG2D (1D11, 10 μ g/mL) before lysis. Cells were normalized by equal cell number,
586 harvested and lysed in ice-cold Radio-Immunoprecipitation Assay (RIPA) buffer (Sigma-
587 Aldrich, UK), supplemented with protease and phosphatase inhibitors (GE Healthcare,
588 Amersham, UK), during 30 minutes on ice. Cell lysates were processed for immunoblot
589 analysis as described⁶.

590 ***Immunoprecipitation***

591 Human CD8⁺ T cells were separated into CD28⁺/CD28⁻ fractions (to obtain sufficient number
592 of cells for analysis) and stimulated with anti-NKG2D (1D11, 10 μ g/mL) or isotype control, for
593 30 minutes at 4 °C. Lysates from 1x10⁷ cells were prepared with ice-cold HNGT buffer (50
594 mM HEPES, pH 7.5, 150 mM EDTA, 10 mM sodium pyrophosphate, 100 mM sodium
595 orthovanadate, 100 mM sodium fluoride, 10 mg/ml aprotinin, 10 mg/ml leupeptin and 1 mM
596 phenylmethylsulfonyl fluoride), for 30 minutes on ice. Cell lysates were incubated overnight
597 at 4°C with anti-NKG2D antibody (clone 5C6, Santa Cruz) or control antibody, followed by
598 precipitation with 10 μ L of pre-washed protein A/G agarose beads (sc-2003, Santa Cruz) for

3 h at 4°C on a rotary shaker. After extensive washing in HGNT buffer, supernatants were recovered and processed for immunoblot analysis, as described above. Co-Immunoprecipitated proteins were detected after incubation with primary antibodies followed by incubation with mouse anti-rabbit IgG (conformation-specific antibody; L27A9; Cell Signaling) or mouse anti-rabbit IgG light chain (L57A3; Cell Signaling) and by a secondary anti-mouse IgG antibody (7076; Cell Signaling).

Mice

Sesn1^{-/-} and Sesn2^{-/-} mice were described previously⁷. The mouse ageing study was performed at the University of Michigan, where the animal procedures were approved by the Institutional Animal Care & Use Committee and overseen by the Unit for Laboratory Animal Medicine. All mice were rested for at least 10 days before being used for *in vivo* studies. Animals were housed under standard conditions, maintained in a 12 h/12 h light/dark cycle at 22 °C ± 1 °C and given food and tap water *ad libitum* in accordance with United Kingdom Home Office regulations (PPL-P69E3D849) and the NIH guideline.

Murine delayed type hypersensitivity model

Knockout and age-matched (18-month-old) C57BL6J WT control mice were imported from the University of Michigan. Young (~6 weeks) WT mice were purchased separately from Charles River. All mice were male. The methylated BSA (mBSA) delayed type hypersensitivity model was performed as described previously⁵⁰. Mice were sensitized at the base of the tail with a 50 µl injection of mBSA in Freund's complete adjuvant (20 mg/ml solution of mBSA in saline emulsified with an equal volume of Freund's adjuvant containing 4 mg/ml *Mycobacterium tuberculosis* H37Ra, Sigma Aldrich). An immune response was evoked 14 days later by subplantar challenge with 50 µl of mBSA in saline (1 mg/ml). The contralateral paw received a saline-only injection and served as a control. The immune response is reported as the difference in paw swelling between left and right paws as determined using callipers (POCO2, Kroeplin). Mice were sacrificed 7 days post-challenge,

according to Schedule 1, using an increasing concentration of CO₂. Death was confirmed by cervical dislocation. Spleens and inguinal lymph nodes were obtained, weighed and dispersed through a 70 µm followed by a 35 µm sterile cell sieve (*Becton Dickinson*) to yield single cell suspensions. Cell numbers were enumerated by haemocytometer and up to 10⁶ cells were used for polychromatic flow cytometry.

In vivo cytotoxicity

24-month-old knockout (*Sesn1*^{-/-}*Sesn2*^{-/-}*Sesn3*^{+/-}) males were imported from the University of Michigan. Age-matched wild type female C57Bl/6J mice were purchased from Envigo. Natural killer cells were depleted by intraperitoneal injection of 100 µg anti-NK1.1 antibody (PK136, BioXCell) 24 hours before cell challenge. The high Rae-1 expressing myeloma cell line 5TGM was labeled with 5 µM CFSE, while splenocytes stained with 0.5 µM were used as Rae-1⁻ controls. Both cell types were mixed at equal ratios and 2x10⁷ were co-injected i.v. Mice were left for 6 hours before being sacrificed. As a measure of Rae-1 directed killing, the ratio of CFSE^{hi} compared to CFSE^{lo} was used to determine Rae-1⁺ cell retrieval and specific lysis.

Statistical analysis

Statistical analysis was performed using GraphPad Prism version 6.00. Tests were used to determine data distribution and depending on the normality of the data, comparisons were performed using the Student *t* test (for two groups, parametric) or the non-parametric Mann–Whitney U test (for two groups, unpaired) and the Wilcoxon signed rank test (for two groups, paired) with two-tailed *P* values unless otherwise stated. When comparing more than two groups, we used one-way ANOVA (parametric, > 2 groups, unpaired), repeated measures ANOVA (parametric, > 2 groups, paired), Kruskal–Wallis (non-parametric, > 2 groups, unpaired) or Friedman (non-parametric, > 2 groups, paired) tests with post-correction for multiple comparisons, as appropriate. The two-way ANOVA test was used to compare the effects of two independent variables between groups. Linear regression analysis was

performed to generate lines of best fit and correlations between variables were analysed using Pearson's or Spearman's rank correlation coefficient (r). Differences were considered significant when $p < 0.05$ (*), $p < 0.01$ (**), $p < 0.001$ (***) and $p < 0.0001$ (****). Data are presented as means \pm standard error of the mean (SEM) unless otherwise stated.

Data and materials availability

The data that support the findings of this study are available from the corresponding author upon request. The complete microarray dataset is available online from the NCBI Gene Expression Omnibus public repository (GEO accession number GSE98640).

The single cell RNA-seq data are available on EGA (Accession number **TBC**).

References

1. Akbar, A. N., Beverley, P. C. & Salmon, M. Will telomere erosion lead to a loss of T-cell memory? *Nature Reviews Immunology* **4**, nri1440 (2004).
2. Gray, D. A role for antigen in the maintenance of immunological memory. *Nat Rev Immunol* **2**, nri706 (2002).
3. Mitri, D. *et al.* Reversible Senescence in Human CD4⁺CD45RA⁺CD27⁻ Memory T Cells. *The Journal of Immunology* **187**, 2093–2100 (2011).
4. Henson, S. M. *et al.* p38 signaling inhibits mTORC1-independent autophagy in senescent human CD8⁺ T cells. *Journal of Clinical Investigation* **124**, 4004–4016 (2014).
5. Lanna, A., Henson, S. M., Escors, D. & Akbar, A. N. The kinase p38 activated by the metabolic regulator AMPK and scaffold TAB1 drives the senescence of human T cells. *Nature immunology* **15**, 965–72 (2014).
6. Tarazona, R. *et al.* Increased expression of NK cell markers on T lymphocytes in aging and chronic activation of the immune system reflects the accumulation of effector/senescent T cells. *Mechanisms of Ageing and Development* **121**, 77–88 (2001).
7. Lanna, A. *et al.* A sestrin-dependent Erk-Jnk-p38 MAPK activation complex inhibits

immunity during aging. *Nature immunology* **18**, 354–363 (2017).

8. Dunne, P. J. *et al.* Quiescence and functional reprogramming of Epstein-Barr virus (EBV)–specific CD8+ T cells during persistent infection. *Blood* **106**, 558–565 (2005).

9. Pereira, B. I. *et al.* Senescent cells evade immune clearance via HLA-E-mediated NK and CD8+ T cell inhibition. *Nat Commun* **10**, 2387 (2019).

10. Krizhanovsky, V., Yon, M., Dickins, R., Hearn, S., Simon, J., Miething, C., Yee, H., Zender, L., Lowe, S. (2008). Senescence of Activated Stellate Cells Limits Liver Fibrosis *Cell* **134**(4), 657–67.

11. Dominguez, C. X. *et al.* The transcription factors ZEB2 and T-bet cooperate to program cytotoxic T cell terminal differentiation in response to LCMV viral infection. *J Exp Medicine* **212**, 2041–2056 (2015).

12. Kovalovsky, D. *et al.* PLZF Induces the Spontaneous Acquisition of Memory/Effector Functions in T Cells Independently of NKT Cell-Related Signals. *J Immunol* **184**, 6746–6755 (2010).

13. Raberger, J., Schebesta, A., Sakaguchi, S., Boucheron, N., Blomberg, K., Berglöff, A., Kolbe, T., Smith, C., Rülcke, T., Ellmeier, W. (2008). The transcriptional regulator PLZF induces the development of CD44 high memory phenotype T cells Proceedings of the National Academy of Sciences **105**(46), 17919–17924.

14. Liu, D. *et al.* Integrin-Dependent Organization and Bidirectional Vesicular Traffic at Cytotoxic Immune Synapses. *Immunity* **31**, 99–109 (2009).

15. Bernardini, G., Sciumè, G. & Santoni, A. Differential chemotactic receptor requirements for NK cell subset trafficking into bone marrow. *Front Immunol* **4**, 12 (2013).

16. van Lier, R. A., ten Berge, I. J. & Gamadia, L. E. Human CD8(+) T-cell differentiation in response to viruses. *Nature reviews. Immunology* **3**, 931–9 (2003).

17. Rufer, N. *et al.* Ex vivo characterization of human CD8+ T subsets with distinct replicative history and partial effector functions. *Blood* **102**, 1779–1787 (2003).

703 18. Henson, S. M. *et al.* KLRG1 signaling induces defective Akt (ser473) phosphorylation
704 and proliferative dysfunction of highly differentiated CD8⁺ T cells. *Blood* **113**, 6619–6628
705 (2009).

706 19. Plunkett, F. J. *et al.* The Loss of Telomerase Activity in Highly Differentiated
707 CD8⁺CD28[–]CD27[–] T Cells Is Associated with Decreased Akt (Ser473)
708 Phosphorylation. *The Journal of Immunology* **178**, 7710–7719 (2007).

709 20. Henson, S. M., Riddell, N. E. & Akbar, A. N. Properties of end-stage human T cells
710 defined by CD45RA re-expression. *Current Opinion in Immunology* **24**, 476–481 (2012).

711 21. Aktas, E., Kucuksezer, U., Bilgic, S., Erten, G. & Deniz, G. Relationship between
712 CD107a expression and cytotoxic activity. *Cell Immunol* **254**, 149–154 (2009).

713 22. Lanier, L. L. NKG2D Receptor and Its Ligands in Host Defense. *Cancer Immunol*
714 *Res* **3**, 575–582 (2015).

715 23. Wu, J. *et al.* An Activating Immunoreceptor Complex Formed by NKG2D and
716 DAP10. *Science* **285**, 730–732 (1999).

717 24. Upshaw, J. L. *et al.* NKG2D-mediated signaling requires a DAP10-bound Grb2-Vav1
718 intermediate and phosphatidylinositol-3-kinase in human natural killer cells. *Nat*
719 *Immunol* **7**, 524–532 (2006).

720 25. Diefenbach, A. *et al.* Selective associations with signaling proteins determine stimulatory
721 versus costimulatory activity of NKG2D. *Nat Immunol* **3**, ni858 (2002).

722 26. Gilfillan, S., Ho, E. L., Cella, M., Yokoyama, W. M. & Colonna, M. NKG2D recruits two
723 distinct adapters to trigger NK cell activation and costimulation. *Nat Immunol* **3**, ni857
724 (2002).

725 27. Wu, J., Cherwinski, H., Spies, T., Phillips, J. H. & Lanier, L. L. Dap10 and Dap12 Form
726 Distinct, but Functionally Cooperative, Receptor Complexes in Natural Killer Cells. *J Exp*
727 *Medicine* **192**, 1059–1068 (2000).

728 28. Akondy, R. S. *et al.* Origin and differentiation of human memory CD8 T cells after
729 vaccination. *Nature* **552**, 362 (2017).

- 730 29. Akondy, R. S. *et al.* The Yellow Fever Virus Vaccine Induces a Broad and Polyfunctional
 731 Human Memory CD8+ T Cell Response. *The Journal of Immunology* **183**, 7919–7930
 732 (2009).
- 733 30. Wang, X. *et al.* Human invariant natural killer T cells acquire transient innate
 734 responsiveness via histone H4 acetylation induced by weak TCR stimulation. *J Exp*
 735 *Medicine* **209**, 987–1000 (2012).
- 736 31. Mingueneau, M. *et al.* Loss of the LAT Adaptor Converts Antigen-Responsive T Cells
 737 into Pathogenic Effectors that Function Independently of the T Cell
 738 Receptor. *Immunity* **31**, 197–208 (2009).
- 739 32. Wencker, M. *et al.* Innate-like T cells straddle innate and adaptive immunity by altering
 740 antigen-receptor responsiveness. *Nature Immunology* **15**, ni.2773 (2013).
- 741 33. Pawelec, G. Immunosenescence: Role of cytomegalovirus. *Exp Gerontol* **54**, 1–5
 742 (2014).
- 743 34. Khan, N. *et al.* Herpesvirus-Specific CD8 T Cell Immunity in Old Age: Cytomegalovirus
 744 Impairs the Response to a Coresident EBV Infection. *The Journal of*
 745 *Immunology* **173**, 7481–7489 (2004).
- 746 35. Jackson, S. E. *et al.* CMV immune evasion and manipulation of the immune system with
 747 aging. *GeroScience* **39**, 273–291 (2017).
- 748 36. Vallejo, A. N. *et al.* Expansions of NK-like $\alpha\beta$ T cells with chronologic aging: Novel
 749 lymphocyte effectors that compensate for functional deficits of conventional NK cells and T
 750 cells. *Ageing Research Reviews* **10**, 354–361 (2011).
- 751 37. Coppé, J.-P. P. *et al.* Senescence-associated secretory phenotypes reveal cell-
 752 nonautonomous functions of oncogenic RAS and the
 753 p53 tumor suppressor. *PLoS biology* **6**, 2853–68 (2008).
- 754 38. Campisi, J. & di Fagagna, F. Cellular senescence: when bad things happen to good
 755 cells. *Nature Reviews Molecular Cell Biology* **8**, 729–740 (2007).

- 756 39. Baker, D. J. *et al.* Naturally occurring p16Ink4a-positive cells shorten healthy
757 lifespan. *Nature* **530**, 184–189 (2016).
- 758 40. Baker, D. J. *et al.* Clearance of p16Ink4a-positive senescent cells delays ageing-
759 associated disorders. *Nature* **479**, 232–6 (2011).
- 760 41. Sagiv, A. *et al.* NKG2D ligands mediate immunosurveillance of senescent
761 cells. *Aging* **8**, 328–44 (2016).
- 762
- 763 **Methods references**
- 764 42. Callender, L. A. *et al.* Human CD8+ EMRA T cells display a senescence-associated
765 secretory phenotype regulated by p38 MAPK. *Aging Cell* **17**, (2018).
- 766 43. Gérard, S., Sibérel, S., Martin, E., Lenoir, C., Aguilar, C., Picard, C., Lantz, O., Fischer, A.,
767 Latour, S. (2013). Human iNKT and MAIT cells exhibit a PLZF-dependent proapoptotic
768 propensity that is counterbalanced by XIAP *Blood* **121**(4), 614-623.
- 769 44. Wolock, S. L., Lopez, R. & Klein, A. M. Scrublet: computational identification of cell
770 doublets in single-cell transcriptomic data. *bioRxiv*(2018). doi:10.1101/357368
- 771 45. Wolf, F. A., Angerer, P. & Theis, F. J. SCANPY: large-scale single-cell gene expression
772 data analysis. *Genome Biol.* **19**, 15 (2018).
- 773 46. Satija, R., Farrell, J. A., Gennert, D., Schier, A. F. & Regev, A. Spatial reconstruction of
774 single-cell gene expression data. *Nat. Biotechnol.* **33**, 495–502 (2015).
- 775 47. McInnes, L., Healy, J. & Melville, J. UMAP: Uniform Manifold Approximation and
776 Projection for Dimension Reduction. *arXiv:1802.03426[cs, stat]* (2018).
- 777 48. Park, J.-E., Polanski, K., Meyer, K. & Teichmann, S. A. Fast Batch Alignment of
778 SingleCell Transcriptomes Unifies Multiple Mouse Cell Atlases into an Integrated
779 Landscape. *bioRxiv*(2018). doi:10.1101/397042

49. Allez, M. *et al.* CD4+NKG2D+ T Cells in Crohn's Disease Mediate Inflammatory and Cytotoxic Responses Through MICA Interactions. *Gastroenterology* **132**, 2346–2358 (2007).

50. Trivedi, S. G. *et al.* Essential role for hematopoietic prostaglandin D2 synthase in the control of delayed type hypersensitivity. *P Natl Acad Sci Usa* **103**, 5179–5184 (2006).

Figure legends

Fig. 1: Transcriptional signature of human CD8⁺ T cell subsets

a) Representative image of CD8⁺ T cells gated on CD27⁺CD45RA⁺ T_N cell, CD27⁺CD45RA⁻ T_{CM} cells, CD27⁻CD45RA⁺ T_{EM} cells, and CD27⁻CD45RA⁺ T_{EMRA} cells isolated from the PBMCs from 6 healthy donors. Numbers in gates represent percentages of cells in each subset from a representative donor. Similar results were obtained in other experiments. **b)** Heat map of gene expression of Affymetrix U133 plus 2 microarrays of sorted T_N and T_{EMRA} CD8⁺ T cell subsets, showing downregulated (in yellow) and upregulated genes (in blue). **c)** The relative fold-change (log₁₀) of differentially expressed genes of interest in T_{CM}, T_{EM} and T_{EMRA} CD8⁺ T cell subsets compared to T_N CD8⁺ T cells. The list of genes of interest is shown in Supplementary table 2 and the complete list of differentially expressed genes from the whole-transcriptome analysis (≥2-fold change, p<0.05, FDR<0.05%) is available in Supplementary table 1. **d)** NKR expression T_N, T_{CM}, T_{EM}, and T_{EMRA} CD8⁺ T cells assessed by flow cytometry on PBMCs from 22 healthy donors (median age = 52, range 25-83). **e)** Representative immunoblots of proximal TCR components Lck, PLCγ1, LAT and Zap70 on CD27⁺CD28⁺, CD27⁺CD28⁻ and CD27⁻CD28⁻ CD8⁺ T cells freshly isolated from PBMCs using magnetic activated cell. Similar data were obtained in 4 independent experiments. Summary data (n = 4) of Lck, Zap70, PLCγ1 and LAT expression normalized to the loading control (GAPDH) and presented relative to the basal expression in CD27⁺CD28⁺ cells set to 1. **d)** Two-way ANOVA with Dunnett's post-test correction and **e)** one-way ANOVA with Tukey's correction (*p < 0.05, **p < 0.01, ***p < 0.001, ****p < 0.0001).

Fig. 2: Single cell RNA-seq (scRNA-seq) of T_N and T_{EMRA} CD8⁺ T cells

a) UMAP plot representing the putative identity of each CD8⁺ T cell cluster. Each colour

represents a cluster. **b)** UMAP plot representing clustering of IL7-R⁺ (in green) and IL7-R⁻ (in purple) CD8⁺ T cells as identified during sorting. **c)** UMAP plots representing expression values of selected genes. Other aliases or CD numbers of proteins encoded by the listed genes are shown in brackets.

Fig. 3: NK and senescence markers within T_N and T_{EMRA}

a) Highlighted clusters were considered as T_N (C0, C4 and C8) and T_{EMRA} (C1, C2 and C6) compartments. **b)** A second round of clustering on the selected groups (n = 39,634 cells) was performed. UMAP plots representing the expression values of **c)** NK and **e)** senescence-associated genes are shown. Other aliases or CD numbers of some gene products are shown in brackets. **d)** NK and **f)** senescence scores were calculated based on the average normalized expression of each gene across T_N and T_{EMRA} compartments (gene lists in Supplementary table 4).

Fig. 4: NKG2D-DAP12 complex mediates NK cytotoxicity in CD27⁺CD28⁻CD8⁺ T cells

a) Cell-surface expression of CD107a detected by flow cytometry was used as a proxy of cytotoxic activity after 6 hour incubation with MHC1-deficient K562 cells (E:T ratio 2:1) of CD27⁺CD28⁺CD8⁺ (DP), CD27⁺CD28⁻CD8⁺ (SP), CD27⁻CD28⁻CD8⁺ (DN), and CD3⁺CD56⁺ NK cells isolated from healthy donors (median and range, n = 5). **b)** CD107a expression on CD28⁻CD8⁺ T cells transfected with NKG2D siRNA (siNKG2D) or control siRNA (siCtrl) and cultured with C1R-MICA or C1R (E:T ratio 2:1) for 6 hours (mean and s.e.m., n = 4). **c)** Immunoblots (representative of five independent experiments with similar results) and **d)** flow cytometry (means and s.e.m., n = 12) showing DAP12 expression on DP, SP, DN CD8⁺ T, and NK cells. **g)** Representative immunoblot of DAP12 from lysed CD28⁺CD8⁺ and CD28⁻CD8⁺ T cells co-immunoprecipitated with anti-NKG2D. Detection of light-chain IgG (IgGL) served as a loading control. Whole-cell lysate immunoblot shown as a control. Representative of two independent experiments. **f)** Phosphorylation of Zap70(Tyr319)/Syk(Tyr352) in freshly isolated CD27⁺28⁻ CD8⁺ T cells after anti-CD3 (OKT3, 10 µg/mL) and/or anti-NKG2D (1D11, 5 µg/mL) stimulation. Numbers indicate relative expression normalized to total Zap70. Representative of 2 experiments. **g)** Granzyme B expression (left) and IFN-γ secretion (right) in DP, SP and DN CD8⁺ T cells after stimulation with anti-NKG2D (5 µg/mL, means and s.e.m., n = 15 donors). **h)** CD107a was assessed by flow cytometry on human CD28⁻CD8⁺ T cells, transfected with DAP12 siRNA (siDAP12) or control siRNA (siCtrl) cultured with C1R-MICA*008 or C1R cells for 6 hours (E:T ratio 2:1; means and s.e.m., n = 4). Statistical significance determined with Kruskal-Wallis test in **a)** Friedman test with Dunn's correction in **d)**, two-way ANOVA with Bonferroni correction in **b**,

844 **j)** and one-way ANOVA with Tukey's in **g)** (* $p < 0.05$, ** $p < 0.01$, *** $p < 0.001$).

845 **Fig. 5: Sestrins and Jnk MAPK dampen TCR signalling in CD27⁺CD28⁺CD8⁺ T cells**

846 Proximal TCR signalling was assessed in CD27⁺CD28⁺CD8⁺ (DP), CD27⁺CD28⁻CD8⁺ (SP),
847 and CD27⁻CD28⁻CD8⁺ (DN) T cells following TCR crosslinking with anti-CD3 (OKT3, 10
848 µg/mL). Representative histograms and summary data (means and s.d., n = 8) of **a)** CD3ζ
849 and **b)** Zap70/Syk phosphorylation are shown. Numbers on histograms represent the mean
850 fluorescence intensity (MFI) for each subset. Light grey histograms represent unstimulated
851 controls. Summary results presented as the MFI relative to that of DP CD8⁺ T cells, set to 1.
852 Protein expression determined by flow cytometry of **c)** Sestrin 1 (Sesn1) and **d)** Sestrin 2
853 (Sesn2) expression in DP, SP, and DN CD8⁺ T cell subsets (means and s.d., n = 10). **e)**
854 Immunoblot image, representative of three independent experiments with similar results, of
855 Sesn2 and phospho-Jnk (T183/Y185) on DP, SP, and DN CD8⁺ T cell subsets. Densitometry
856 data from western blots for all donors is also shown (means and s.e.m., n = 3-4). Statistical
857 significance determined with ANOVA with Friedman test and Dunn's post-test correction in
858 **a-b)**, repeated measures one-way ANOVA with Tukey's multiple comparisons test in **c-e)** (* p
859 < 0.05 , ** $p < 0.01$, *** $p < 0.001$, **** $p < 0.0001$).

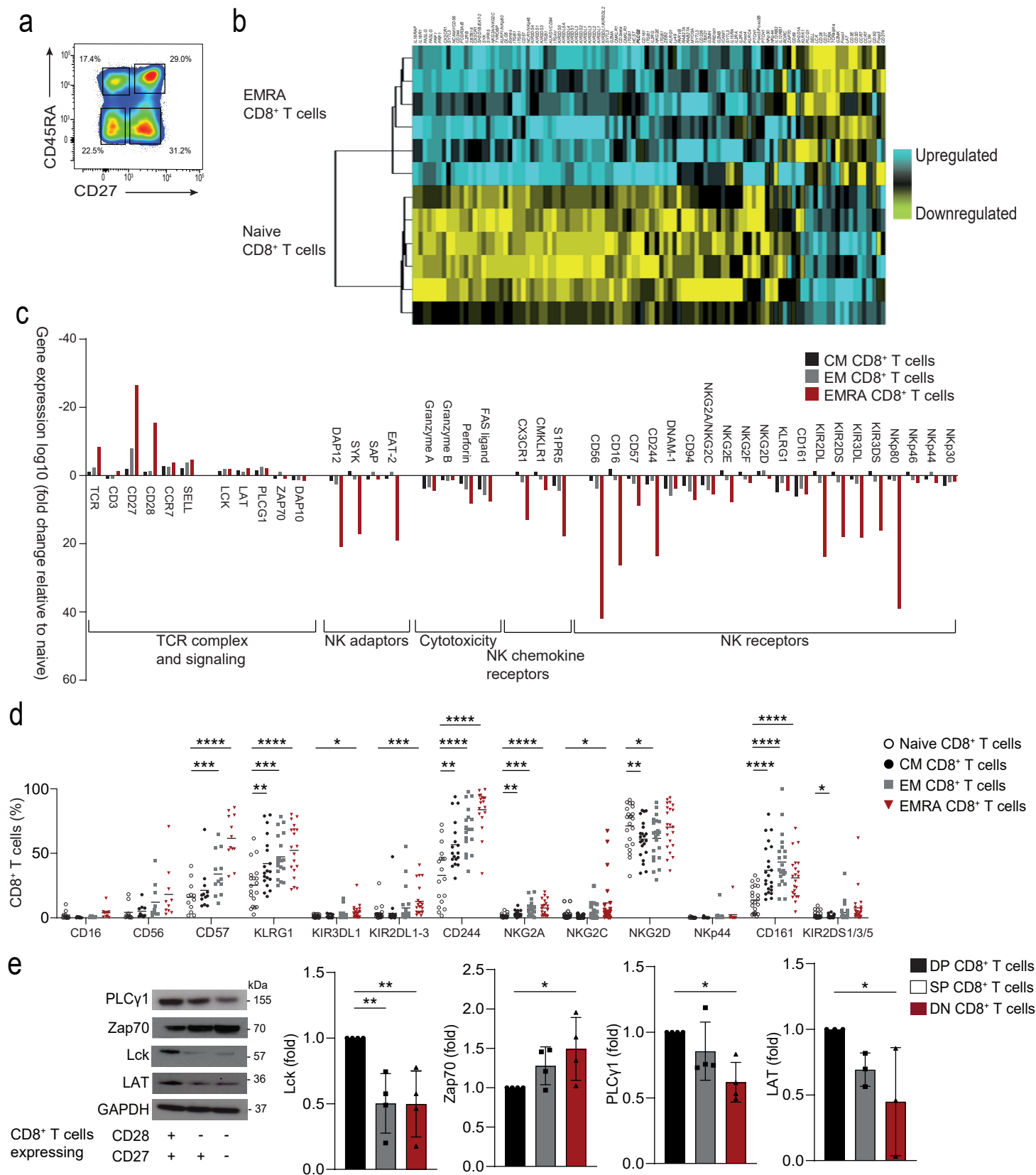
860 **Fig. 6: Sestrins regulate DAP12 and NKG2D expression in CD8⁺ T cells.**

861 **a)** Representative immunoblot of co-immunoprecipitation with anti-NKG2D of lysed CD28⁺
862 and CD28⁻ CD8⁺ T cells showing DAP12, Sesn2 and P-Jnk (T183/Y185) expression.
863 Detection of IgG light chain (IgGL) in immunoprecipitate blots (IP) served as loading control.
864 Results are representative of 2 independent experiments. **b)** Representative images of
865 imaging cytometry of Sesn2 (AF488, green), DAP12 (PE, red) and P-Jnk (T183/Y185,
866 AF647, yellow) single stain controls as well as triple-stained CD27⁺CD28⁺ (DP) and CD27⁻
867 CD28⁻ (DN) CD8⁺ T cells. Nuclei are stained with DAPI (blue). Scale bars – 7 µm. **c)** Bright
868 Detail Similarity score to determine overlap of Sesn2 and DAP12 or P-Jnk in CD28⁺ and
869 CD28⁻ CD8⁺ T cells. Values exceeding 2 were considered to be overlapping. Data are
870 normalized to the DP subset for each donor (means and s.d., n = 6). **d-e)** Isolated human
871 CD8⁺CD28⁻ T cells were transduced with control (shCtrl) or anti-sestrin (shSesn) vectors. **d)**
872 Representative immunoblot for Sesn2 and DAP12 (representative of two experiments). **e)**
873 Representative contour plots and summary data of NKG2D expression. Results are
874 presented relative to cells transduced with shCtrl for each donor, set as 1 (means and s.d., n
875 = 3 donors). **f)** Frequency of NKG2D and CD28 expressing cells after Jnk inhibition by
876 siRNA in CD28⁻CD8⁺ T cells (means and s.d., n = 6 donors). P-Lck detection by flow
877 cytometry of CD28⁻CD8⁺ T cells pre-treated with Jnk inhibitor (SP-600125, 10 µM) prior to

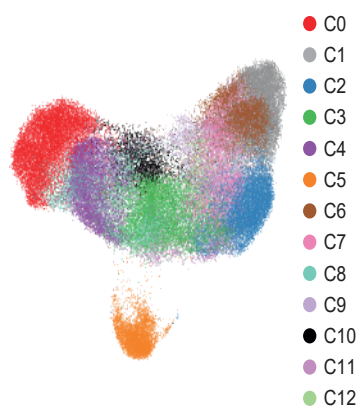
878 anti-CD3 stimulation (OKT3, 10 µg/ml; means and s.d., n = 8 donors). Two-tailed paired
879 Student's *t* tests in **c,f-g** (**p* < 0.05, ***p* < 0.01, ****p* < 0.001).

880 **Fig. 7: Sestrins induce an age-dependent NK phenotype in CD8⁺ T cells *in vivo***

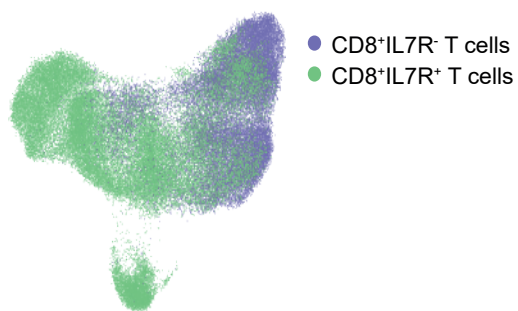
881 **a)** Time course of paw size (normalized to the contralateral, PBS control paw) following DTH
882 challenge (at time = 0 h) and **b)** the overall response assessed as the integration of the time
883 course data (means and s.d., n = 4 young wild-type (Y WT), 10 old wild-type (O WT), 5 old
884 *Sesn1*^{-/-} (O *Sesn1*^{-/-}), and 4 old *Sesn2*^{-/-} (O *Sesn2*^{-/-}) mice. **c)** Representative pseudo-colour
885 density plots for young wild-type (white), old wild-type (black), old *Sesn1*^{-/-} (grey), and old
886 *Sesn2*^{-/-} (red) mice showing CD44 vs NKG2D expression. Frequencies of parent gates are
887 shown in the top right-hand corner. The frequency of NKG2D expression in **d)**
888 TCRβ⁺CD3⁺CD8⁺ T cells, **f)** NK1.1⁺NK cells, and **g)** TCRβ⁺CD3⁺CD1d-tet⁺ invariant NKT
889 (iNKT) cells was assessed by flow cytometry (n = 3 mice per group). **e)** Representative
890 histogram of DAP12 expression in TCRβ⁺CD3⁺CD8⁺ T cells with summary expression data
891 (n = 3 per group, n = 1 young wild-type). **h)** Retrieval, 6 hours post-injection of CFSE-
892 labelled Rae-1⁺ 5TGM1 cells from NK-depleted (24h, anti-NK1.1 i.p.) old wild-type (WT) and
893 old *Sesn1*^{-/-}*Sesn2*^{-/-}*Sesn3*^{+/+} (KO) mice (means and s.d., n = 3 mice per group). **i)** Specific
894 lysis of Rae-1⁺ 5TGM1 cells *in vivo* (n = 3 mice per group). Statistical significance
895 determined with one-way ANOVA with Tukey's multiple comparisons test in **b,d-g**; two-
896 tailed unpaired Student's *t* tests in **h-i**). (**p* < 0.05, ***p* < 0.01, ****p* < 0.001, *****p* < 0.0001).



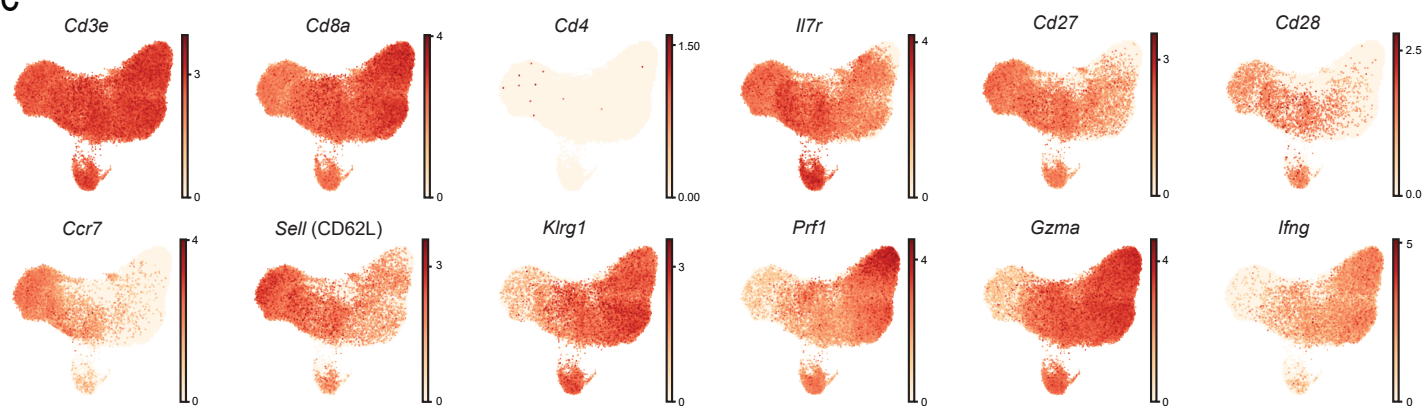
a



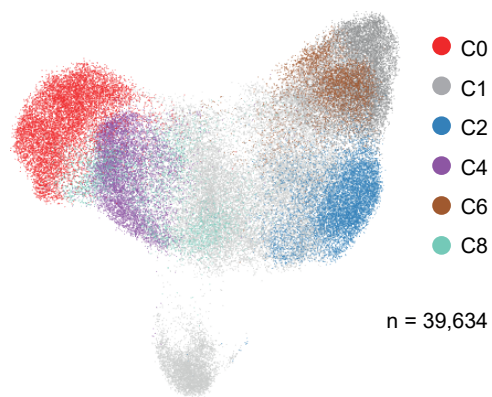
b



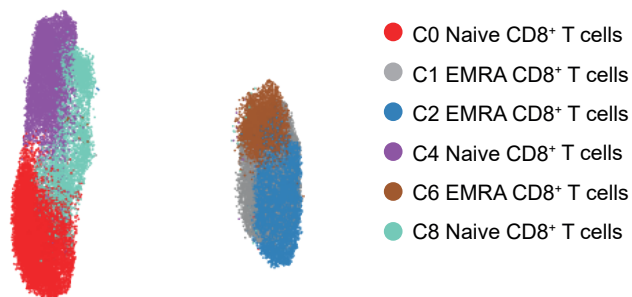
c



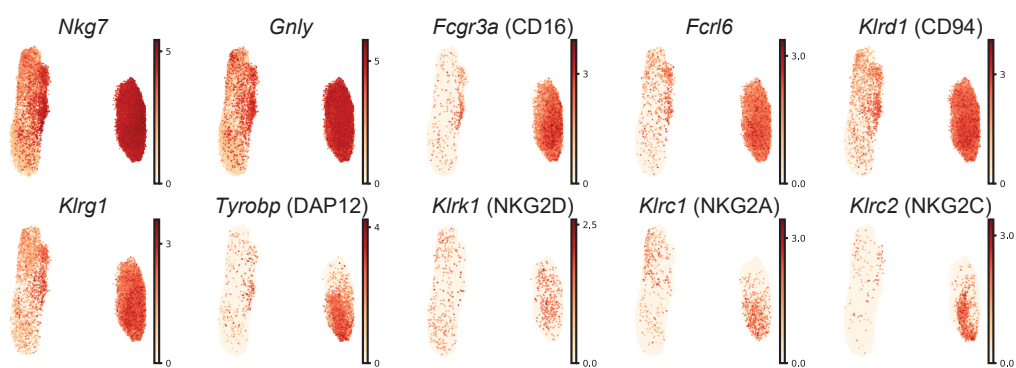
a



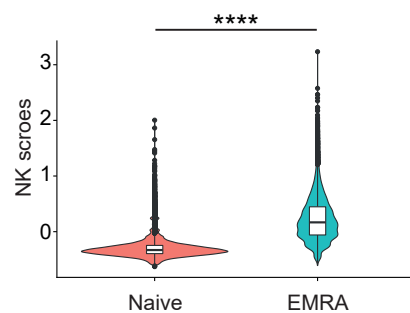
b



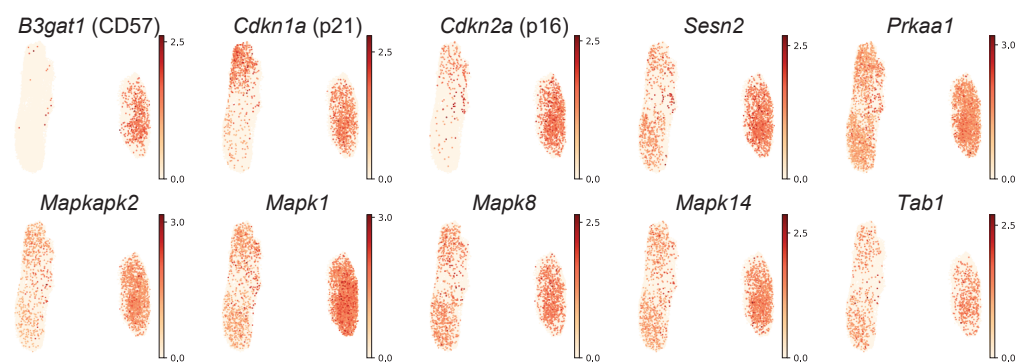
c



d



e



f

